Efficient and individually controllable mechanisms for mode and polarization selection in VCSELs, based on a common, localized, sub-wavelength surface grating

Johan S. Gustavsson, Åsa Haglund, Josip A. Vukušić, Jörgen Bengtsson, Piotr Jedrasik, and Anders Larsson

Department of Microtechnology and Nanoscience, Chalmers University of Technology, SE-41296, Gothenburg, Sweden

johan.gustavsson@mc2.chalmers.se

Abstract: We have theoretically investigated the combined fundamental-mode and polarization selection in 850-nm oxide-confined vertical-cavity surface-emitting lasers (VCSELs) using a locally etched sub-wavelength surface grating. The physical mechanisms behind the selection are, first, the strongly polarization sensitive effective refractive index of the volume occupied by the grating structure, and second, the dramatic change of the reflectivity of a multi-layer Bragg mirror that can occur by simply changing the refractive index of the outermost layer. For a VCSEL cavity this layer is the surface layer and its refractive index is changed by the introduction of the sub-wavelength grating; in this case the grating leads to a higher reflectivity for the desired polarization. By localizing the surface grating area to a carefully chosen region near the optical axis it is therefore possible to ensure that the fundamental mode experiences a high reflectivity, or low cavity loss, while other modes experience more of the low-reflectance region of the peripheral part of the Bragg mirror and thus suffer higher loss. Cold-cavity calculations on a VCSEL with oxide aperture and grating region diameters of 4.5 μm and 2.5 μm, respectively, indicate that a loss difference of $\sim$20 cm^{-1} between the fundamental mode and the first higher order mode can be obtained simultaneously with an orthogonal polarization mode discrimination of $>$15 cm^{-1}. Based on previous experience, these values should enable robust single-mode operation with only the desired polarization orientation. What is also important, for the lasing mode the introduction of a sub-wavelength grating has no detrimental effect, so its characteristics, such as threshold current, slope efficiency, and far-field profile are unaffected. Moreover, since the effective index is a result of an averaging over several sub-wavelength grating periods, it is fairly insensitive to the detailed shape of the grating grooves, which should relax the fabrication tolerances.

OCIS codes: (230.0250) Optoelectronics; (250.7260) Vertical cavity surface emitting lasers

#8151 - $15.00 USD Received 15 July 2005; revised 15 August 2005; accepted 16 August 2005

References and links

1. H. J. Unold, M. C. Riedl, S. W. Z. Mahmoud, R. Jäger, and K. J. Ebeling, "Long monolithic cavity VCSELs for high singlemode output power," Electron. Lett. **37**(3), 178–179 (2001).
2. D. Zhou and L. J. Mawst, "High-power single-mode antiresonant reflecting optical waveguide-type vertical-cavity surface-emitting lasers," IEEE J. Quantum Electron. **38,** 1599–1606 (2002).
3. Å. Haglund, J. S. Gustavsson, J. Vukušić, P. Modh, and A. Larsson, "Single fundamental mode output power exceeding 6 mW from VCSELs with a shallow surface relief," IEEE Photon. Techn. Lett. **16,** 368–370 (2004).
4. S. J. Schablitsky, L. Zhuang, R. C. Shi, and S. Y. Chou, "Controlling polarization of vertical-cavity surface-emitting lasers using amorphous silicon subwavelength transmission gratings," Appl. Phys. Lett. **69,** 7–9 (1996).
5. J.-H. Ser, Y.-G. Ju, J.-H. Shin, and Y. H. Lee, "Polarization stabilization of vertical-cavity top-surface-emitting lasers by inscription of fine metal-interlaced gratings," Appl. Phys. Lett. **66,** 2769–2771 (1995).
6. Y. Hong, R. Ju, S. Spencer, and K. A. Shore, "Investigation of polarization bistability in vertical-cavity surface-emitting lasers subjected to optical feedback," IEEE J. Quantum Electron. **41,** 619–624 (2005).
7. N. Nishiyama, M. Arai, S. Shinada, M. Azuchi, T. Miyamoto, F. Koyama, and K. Iga, "Highly strained GaInAs-GaAs quantum-well vertical-cavity surface-emitting laser on GaAs (311)B substrate for stable polarization operation," IEEE J. Sel. Top. Quantum Electron. **7,** 242–248 (2001).
8. K.-H. Lee, J.-H. Baek, I.-K. Hwang, and Y.-H. Lee, "Square-lattice photonic-crystal vertical-cavity surface-emitting lasers," Opt. Express **12,** 4136–4143 (2004), http://www.opticsexpress.org/abstract.cfm?URI=OPEX-12-17-4136.
9. K. D. Choquette and R. E. Leibenguth, "Control of vertical-cavity laser polarization with anisotropic transverse cavity geometries," IEEE Photon. Techn. Lett. **6,** 40–42 (1994).
10. K. Panajotov, R. Kotynski, M. Camarena, and H. Thienpont, "Modeling of the polarization behavior of elliptical surface-relief VCSELs," Opt. Quantum Electron. **37,** 241–252 (2005).
11. J. M. Ostermann, P. Debernardi, C. Jalics, A. Kroner, M. C. Riedl, and R. Michalzik, "Surface gratings for polarization control of single- and multi-mode oxide-confined vertical-cavity surface-emitting lasers," Opt. Commun. **246,** 511–519 (2005).
12. Å. Haglund, J. S. Gustavsson, J. Vukušić, P. Jedrasik, and A. Larsson, "High-power fundamental-mode and polarization stabilized VCSELs using a sub-wavelength surface grating," Electron. Lett. **41**(14), 37–38 (2005).
13. M. Born and E. Wolf, *Principles of Optics, 4th ed.* (Pergamon Press, Bath, Great Britain, 1970).
14. G. R. Hadley, "Effective index model for vertical-cavity surface-emitting lasers," Opt. Lett. **20,** 1483–1485 (1995).
15. M. A. Afromowitz, "Refractive index of $Ga_{1-x}Al_xAs$," Solid State Comm. **15**(1), 59–63 (1974).
16. D. Kuksenkov and H. Temkin, "Polarization Related Properties of Vertical-Cavity Lasers," in *Vertical-Cavity Surface-Emitting Lasers,* C. Wilmsen, H. Temkin, and L. A. Coldren, eds. (Cambridge University Press, Cambridge, U.K., 1999), pp. 233–267.

1. Introduction

The vertical-cavity surface-emitting laser (VCSEL) is an attractive light source in optical communication applications. The low fabrication costs together with its favorable properties of low threshold current, high efficiency, high bandwidth at low currents, and ability for two-dimensional integration, has made it an established transmitter in short distance parallel fiber-optic links. New applications for the VCSEL are continuously arising, such as in longer distance fiber-optic communication, sensing, laser printing, and optical storage. Many of these applications require single-mode lasers with output powers of several milliwatts, frequently with a stable linear polarization state as an additional requirement. Unfortunately, the VCSEL has a tendency to lase in multiple transverse modes, due to its relatively large transverse dimensions, and often with an unpredictable linear polarization state, due to weak anisotropy of the material properties and lack of asymmetry in the device geometry. Several methods have been developed to achieve single-mode emission in VCSELs, such as using an extended cavity [1], anti-resonant reflecting optical waveguides [2], and a circular surface depression [3]. Similarly for polarization control one has used sub-wavelength gratings in amorphous silicon [4], metal-interlaced gratings [5], external feed-back [6], and epitaxial growth on non-(100) GaAs substrates [7]. However, only a few methods have been developed for combined mode and polarization selection. These include photonic crystal patterns [8], asymmetric air-post structures [9], elliptical

#8151 - $15.00 USD Received 15 July 2005; revised 15 August 2005; accepted 16 August 2005

surface depressions [10], and locally etched surface gratings. In the latter method, a grating with a period larger than the optical wavelength in the material has been presented [11], and recently we have experimentally demonstrated the successful use of a sub-wavelength grating [12]. A locally etched surface grating allows for the use of a relatively large oxide aperture, which reduces device resistance and thereby self-heating, enabling higher output powers. The advantage of using a sub-wavelength grating compared to a larger grating period is that the diffraction related losses and beam degradation should be minimized. However, the fabrication of these sub-wavelength gratings is apparently more challenging since it requires high-resolution definition.

In this work, we have performed numerical calculations to investigate the achievable mode and polarization selection in 850-nm oxide-confined VCSELs with a locally etched sub-wavelength surface grating. We also investigate how sensitive the mode and polarization selection are to the grating geometry, which gives information on the fabrication tolerances. In Section 2 the basic polarization dependent properties of a sub-wavelength surface grating etched in GaAs are first discussed. Then the combined mode and polarization selection in a VCSEL structure, where the grating region diameter is smaller than the oxide aperture diameter, is analyzed. In Section 3 the technique is experimentally demonstrated, and in Section 4 a conclusion is given.

2. VCSEL surface structures for polarization and mode selection

2.1. Sub-wavelength grating etched in GaAs

A sub-wavelength grating has a periodicity that is shorter than the optical wavelength in the material. No diffraction orders are therefore introduced. The electrical field of the wave polarized parallel or perpendicular to the grooves experiences the grating as a homogeneous medium, but with different effective indices, see Fig. 1(a). This effect has been used to produce anti-reflecting surfaces, birefringent elements, filters, and polarizers. Advantages of using a sub-wavelength grating for these applications include that the effective index can be tailored and a high effective index contrast between the two orthogonal polarization states can be achieved. The anisotropic effective index can be approximately computed analytically by simple boundary condition considerations and spatial weighting of the electrical and displacement fields [13],

$$\begin{aligned} \varepsilon_{\mathrm{eff}\parallel} &= 1 + d(\varepsilon - 1) \\ \varepsilon_{\mathrm{eff}\perp} &= \frac{\varepsilon}{d + \varepsilon(1-d)}, \end{aligned} \tag{1}$$

where ε is the dielectric constant of the grating material and d is the duty cycle, which is defined as the ridge to period ratio, see Fig. 1(a). It is assumed that the grating is terminated into air. The effective index approximation becomes less accurate as the grating period approaches the optical wavelength. We therefore compared with $\varepsilon_{\mathrm{eff}}$-values obtained using the two-dimensional finite-difference-time-domain (FDTD) method. In this case $\varepsilon_{\mathrm{eff}}$ was calculated by matching the phase of the reflection from a plane wave incident on the sub-wavelength grating to that of a plane wave incident on a homogeneous slab. Fig. 1(b) shows the anisotropic effective index versus duty cycle at 840 nm, for a sub-wavelength grating etched in GaAs. The solid lines represent the analytical values from Eq. (1), the squares and triangles the FDTD values for a grating period that is one-fifth and one-half, respectively, of the wavelength in GaAs. For the parallel polarization the agreement is excellent but for the perpendicular polarization the FDTD values are not quite as low, resulting in a somewhat smaller index difference, however they approach the analytical values as the grating period is reduced. Of course, the fabrication of a sub-wavelength grating becomes more challenging as the period is reduced. At 840 nm the

#8151 - $15.00 USD Received 15 July 2005; revised 15 August 2005; accepted 16 August 2005

optical wavelength in GaAs is ∼240 nm which means that the squares and triangles correspond to a grating period of 48 and 120 nm, respectively. To summarize, the effective index values indicate a promising difference between the two orthogonal polarization directions, accentuated for shorter grating periods, particularly for a duty cycle between 50 and 80%.

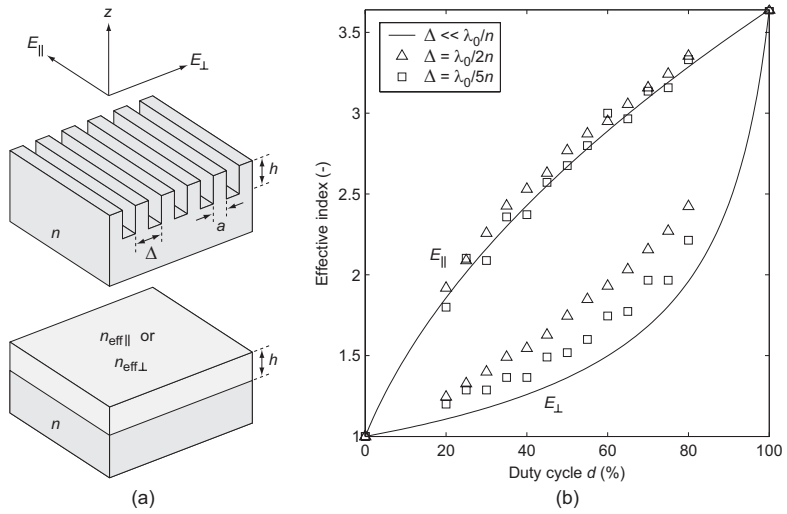

Fig. 1. (a) A sub-wavelength grating with period Δ and ridge width *a*, and its effective index equivalent for a plane wave propagating in the *z*-direction. (b) Effective index in GaAs as a function of duty cycle $d=a/\Delta$ at a free-space optical wavelength (λ_0) of 840 nm.

2.2. VCSEL cavity and lateral extent of grating area

The investigated oxide-confined VCSEL is designed for top emission at 850 nm wavelength and is schematically shown in Fig. 2 together with a scanning electron microscope (SEM) image of a sub-wavelength test grating. The standard 1-λ cavity epitaxial structure consists of an active region with three GaAs/$Al_{0.3}Ga_{0.7}As$ quantum wells and a top p-doped and bottom n-doped DBR of 22 and 34 $Al_{0.9}Ga_{0.1}As/Al_{0.12}Ga_{0.88}As$ mirror pairs, respectively. To reduce the mirror resistance while maintaining a low free-carrier absorption loss, graded interfaces and modulation doping were applied. A 30-nm-thick high aluminium content layer, positioned at the bottom of the top DBR (close to a node of the longitudinal standing-wave intensity distribution) is used to form the oxide aperture. For the mode and polarization control an ”inverted” sub-wavelength surface grating is used: a quarter-wavelength-thick topmost GaAs layer is added to the epitaxial structure to introduce anti-phase reflections, which dramatically increases the top mirror loss; a sub-wavelength surface grating is then etched in a circular region into the top mirror to locally restore the low mirror loss for the fundamental mode with a polarization state perpendicular to the grating grooves. This inverted technique has fabricational advantages since it lowers the required precision of the etch depth *h* of the grating grooves.

The scalar method originating from Hadley [14] has frequently been used to numerically calculate the optical fields in oxide-confined VCSELs, which are normally characterized by near-paraxial propagation with linear polarization states lying in the plane of the epitaxial layers (normally switching between the [011] and the [$0\bar{1}1$] crystallographic directions). In our work we can use this method since the optical fields experience the volume occupied by the sub-wavelength grating as a homogeneous material. In Hadley’s method, the longitudinal and transverse dependencies of the electric field are separated. The longitudinal variation of the field

#8151 - $15.00 USD Received 15 July 2005; revised 15 August 2005; accepted 16 August 2005

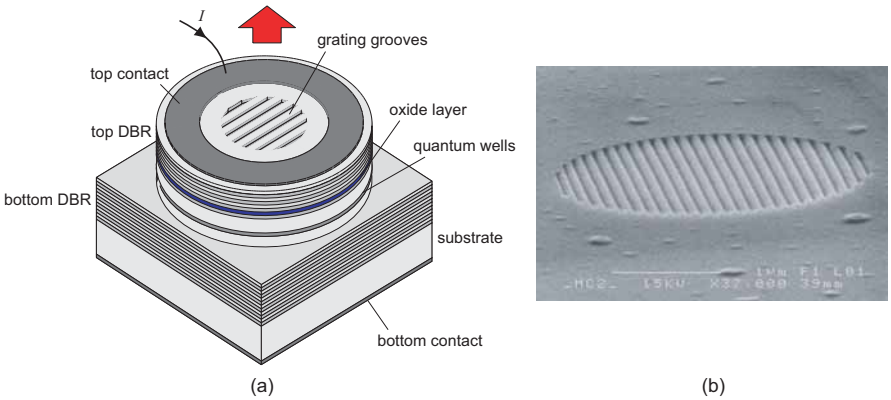

Fig. 2. (a) Schematic illustration of the VCSEL structure and (b) an SEM image of a test grating with period 120 nm etched in bulk GaAs, with a lateral extent typical for a VCSEL with a surface grating.

is computed from an eigenvalue equation, where the real and imaginary part of the eigenvalue are related to a cavity effective index and cavity loss, respectively. This is done for all separate transverse regions. The results are then input to another eigenvalue equation for the transverse variation of the field. The real and imaginary part of this eigenvalue are related to the modal wavelength and modal loss, respectively. The Afromowitz model [15] was applied to compute the refractive index for the different AlGaAs compositions in the epitaxial structure.

Near the optical axis, where the sub-wavelength grating is etched, the cavity-loss is polarization sensitive. Figure 3(a) shows the calculated cavity loss in this region for $E_{\parallel}$ versus etch depth and duty cycle. The solid and dotted lines represent calculations using the analytical ($\Delta << \lambda_0/n$) and FDTD ($\Delta = \lambda_0/2n$) values, respectively, for the effective index of the grating. For zero duty cycle, which corresponds to a completely etched surface, the loss decreases rapidly with etch depth reaching a broad minimum at the quarter-wavelength-depth of $\sim$60 nm. When the duty cycle is increased the loss contrast between zero and 60-nm etch depth decreases significantly. This is in contrast to $E_{\perp}$ for duty cycles up to $\sim$80%, which is shown in Fig. 3(b), and is a result of the effective index of the grating in this case being much closer to the index of air. Figure 3(c) shows the loss difference between the two orthogonal polarization states, calculated from the results in Fig. 3(a) and 3(b). A loss difference of $\sim$20-40 cm^{-1} is achieved at 60-nm etch depth for a duty cycle of 50-80%, even for a grating period as large as $\Delta = \lambda_0/2n$. Also note that the favored polarization can be switched by etching deeper, with a high loss contrast at the half-wavelength-depth of $\sim$120 nm.

The optical modes in the VCSEL are guided by the oxide aperture. By etching a $\sim$60-nm-deep sub-wavelength surface grating, concentric with the oxide aperture, in a circular region with a diameter smaller than the diameter of the oxide aperture, strong fundamental-mode and polarization selection can simultaneously be achieved. The higher-order mode discrimination is a result of their larger overlap with the high-mirror loss area outside the grating region, while the polarization pinning of the fundamental mode is a result of the polarization dependent mirror losses inside the grating region. The combined mode and polarization selectivity depends strongly on the diameter of the grating region and the oxide aperture. Now taking the full transverse structure of the VCSEL into account, the calculated cavity loss for the fundamental-mode (LP01) and the first higher-order mode (LP11), being the two most relevant modes, versus duty cycle for a 4.5 μm oxide aperture VCSEL with an optimized grating region diameter of 2.5 μm

#8151 - $15.00 USD Received 15 July 2005; revised 15 August 2005; accepted 16 August 2005

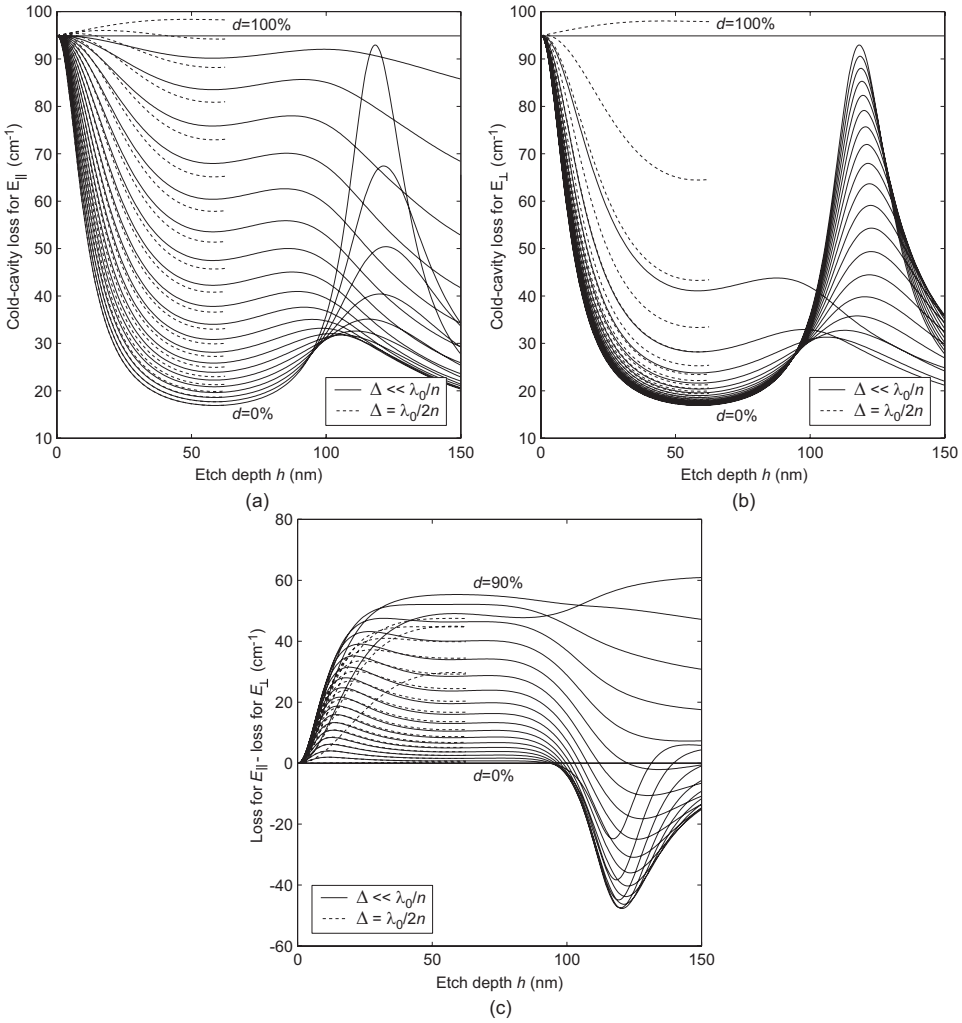

Fig. 3. (a) Cavity loss for $E_{\|}$, (b) cavity loss for $E_{\perp}$, and (c) loss difference, loss for $E_{\|}$ - loss for $E_{\perp}$, as a function of grating etch depth and duty cycle.

is shown in Fig. 4(a). The grating etch depth is 60 nm. The loss for the LP01-mode and its difference to the LP11-mode, both with the favored perpendicular polarization, do not change significantly for duty cycles up to ∼80% (a duty cycle above 80% is furthermore very difficult to fabricate). This implies that the threshold current, slope efficiency, resonant frequency, and mode selectivity would not degrade compared to a completely etched region (d=0%). The case of d=0% corresponds to a conventional disk-shaped surface depression, which has proven to yield a single-fundamental-mode VCSEL with an output power exceeding 6 mW [3], albeit with an uncontrolled polarization. From our experience a high mode selectivity, typically $>$15 cm^{-1}, is required to achieve a dynamic single-mode VCSEL. Further, the figure also shows that the polarization selectivity increases rapidly with duty cycle. In Ref. [16], a loss difference of at least 10 cm^{-1} between the two orthogonal states was stated to be the requirement for achieving a polarization-stable VCSEL also under dynamic operation. The figure shows that a 60-80% duty cycle yields a very promising mode and polarization selectivity of ∼20 and $>$15 cm^{-1},

#8151 - $15.00 USD Received 15 July 2005; revised 15 August 2005; accepted 16 August 2005

respectively, even where the grating period is as large as $\Delta=\lambda_0/2n$. Figure 4(b) shows the calculated modal cold-cavity loss versus grating etch depth for the same device geometry as in Fig. 4(a), with a fixed grating duty cycle of 60%. For etch depths within 20 nm from the targeting etch depth of 60 nm the modal losses change negligibly. Thus, for duty cycles between 60 and 80% and etch depths between 40 and 80 nm a high combined mode and polarization selection can be achieved while maintaining a low loss for the selected LP01-mode with perpendicular polarization.

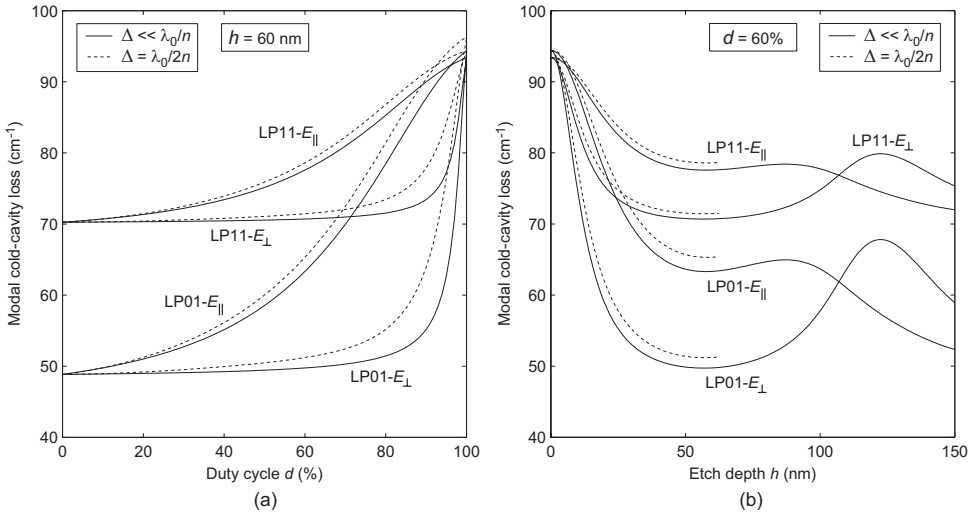

Fig. 4. (a) Modal loss as a function of grating duty cycle for a VCSEL with a 60-nm grating etch depth and (b) modal loss as a function of grating etch depth for a VCSEL with a 60% duty cycle. The oxide aperture is 4.5 μm and the grating region diameter is 2.5 μm.

3. Experimental results

To experimentally demonstrate the efficiency of the selection mechanisms we have fabricated the above theoretically investigated VCSELs with the mentioned inverted sub-wavelength surface grating. The epitaxial structure was provided by IQE Europe Ltd. and the gratings were fabricated using electron beam lithography and reactive ion beam etching. Figure 5 shows polarization resolved light-current characteristics, optical spectra, and far-field for two VCSELs having a grating with a period Δ=120 nm, a duty cycle d=60%, and an etch depth h=60 nm. The grating grooves are oriented in the $[0\bar{1}1]$ crystallographic direction in VCSEL (a) and in the perpendicular [011] direction in VCSEL (b). As shown, both lasers are single-mode (side-mode-suppression-ratio, SMSR, of $>$30dB) and polarization stable (orthogonal-polarization-suppression-ratio, OPSR, of $\sim$20dB) from threshold up to thermal roll-over, reaching 4.1 mW of output power. The polarization state is in both cases perpendicular to the grating grooves, i.e. it rotates with the orientation of the grating. Moreover, there is no indication of beam degradation, i.e. side-lobes, in the far-field introduced by the grating. To verify that the combined mode and polarization selection indeed stems from the sub-wavelength grating and that it does not significantly affect other important laser characteristics we further fabricated two VCSELs with the same geometry as VCSELs (a) and (b) apart from one having no sub-wavelength surface grating and no quarter-wavelength thick topmost anti-phase layer (i.e. a conventional multimode VCSEL), referred to as VCSEL (c) and the other having a 0% duty cycle (i.e. a disk-shaped surface depression), referred to as VCSEL (d). VCSEL (c) was found to be mul-

#8151 - $15.00 USD Received 15 July 2005; revised 15 August 2005; accepted 16 August 2005

timode with 2 to 4 transverse modes depending on the current, and has an OPSR that varies unpredictably between 0 and 10dB from threshold up to thermal roll-over. VCSEL (d) was single-mode, however the polarization state switches at a drive current twice the threshold current and again at the thermal roll-over. The threshold current, initial slope efficiency, and maximum output power are 0.23 mA, 0.67 W/A, and 4.1 mW for VCSEL (c) and 0.26 mA, 0.73 W/A, and 3.8 mW for VCSEL (d), which is very similar to the values for VCSELs (a) and (b), supporting our numerical results. For more details on the experimental results see [12].

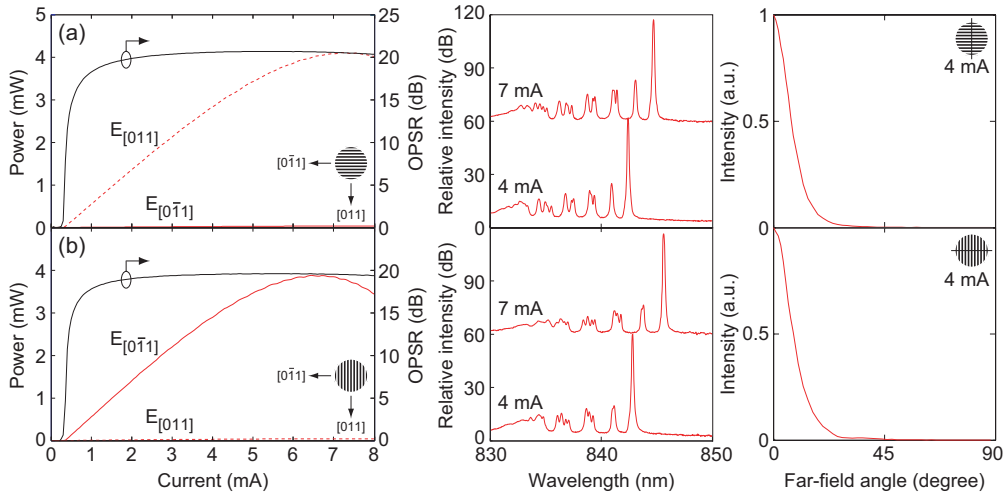

Fig. 5. Output power (polarization resolved) and OPSR versus current, optical spectra, and far-field, for a VCSEL with a sub-wavelength surface grating along (a) the [01$\bar{1}$] direction, and (b) along the [011] direction. The oxide aperture diameter is 4.5 μm, the grating region diameter is 2.5 μm, the grating duty cycle is 60%, and the grating etch depth is 60 nm.

4. Conclusion

We have performed numerical calculations to study the combined fundamental-mode and polarization selection in 850-nm oxide-confined VCSELs with a sub-wavelength surface grating etched in a circular region, which has a diameter that is smaller than the oxide aperture. Essentially, it is the spatial extension of the grating region that determines the mode selection while the orientation of the grating grooves are responsible for the polarization selection. The physical interaction of the optical field with the sub-wavelength grating is very different from that of a grating with a period larger than the optical wavelength in the material. The optical field experiences the sub-wavelength grating as an anisotropic homogeneous medium, which makes it possible to produce a polarization sensitive mirror loss that does not introduce any diffraction losses nor side-lobes in the far-field. From cold-cavity calculations we demonstrate that for a VCSEL with a 4.5 μm oxide aperture diameter and a 2.5 μm grating region diameter, a loss difference of as high as $\sim$20 cm^{-1} between the LP01- and LP11-modes, and a loss difference exceeding 15 cm^{-1} between the two orthogonal polarization states of the LP01-mode, can simultaneously be achieved for grating duty cycles between 60 and 80% and grating etch depths between 40 and 80 nm. This comes without significantly affecting other important laser characteristics. Fabricated VCSELs with a 60% duty cycle and 60 nm etch depth were single-mode and polarization stable from threshold up to thermal roll-over, producing 4.1 mW of output power. No notable degradation in threshold current, slope efficiency, and beam quality was

#8151 - $15.00 USD Received 15 July 2005; revised 15 August 2005; accepted 16 August 2005

observed compared to VCSELs without a sub-wavelength surface grating, which supports our numerical results.

Although the physical selection mechanisms in these VCSELs seem to work well indeed, one might be concerned about how practical they are for large-volume production, since fabricating sub-wavelength gratings requires a high resolution definition. In our experimental work we used electron beam lithography and subsequent reactive ion beam etching. Electron beam lithography is notorious for its high cost in large-area writing. However, since the grating area is small the electron beam exposure time and cost can be kept low. Further, the cold-cavity calculations indicate that the grating duty cycle and grating etch depth can deviate substantially from their target values without affecting the mode and polarization selection. In fact, the fabrication of these sub-wavelength gratings is not necessarily more demanding than for a grating with period larger than the optical wavelength, thanks to their effective index character which lowers the sensitivity for errors in the profile of the grating grooves.

Acknowledgments

This work was supported by the Swedish Foundation for Strategic Research (SSF).

#8151 - $15.00 USD Received 15 July 2005; revised 15 August 2005; accepted 16 August 2005